

Title	Representation of Power-Voltage Characteristics of Induction Motor Load for Power System Stability Studies
Author(s)	Azuma, Yasuhiro; Taniguchi, Tsuneo; Nakamura, Masao
Editor(s)	
Citation	Bulletin of University of Osaka Prefecture. Series A, Engineering and natural sciences. 1973, 21(2), p.253-264
Issue Date	1973-03-31
URL	http://hdl.handle.net/10466/8210
Rights	

Representation of Power-Voltage Characteristics of Induction Motor Loads for Power System Stability Studies

Yasuhiro AZUMA*, Tsuneo TANIGUCHI** and Masao NAKAMURA**

(Received November 15, 1972)

In power system stability studies, the suitable representation of load characteristics under system voltage fluctuation has been required.

In this study, the authors derive theoretically the power-voltage characteristics of induction motor loads which occupy considerable part in the system loads and discuss the appropriateness of using the characteristics for power system stability studies.

1. Introduction

The induction motor's behaviors including the mechanical and rotor electrical transient are originally expressed by nonlinear differential equations⁽¹⁾⁻⁽³⁾. In some case, however, where the terminal voltage variation of an induction motor is not so wide, it can be derived from the familiar steady-state equivalent circuit that the relation between it's power and voltage is approximately linear.

The authors attempt to apply this relation to the representation of the induction motor's behaviors under the transient state of power system.

Appropriateness of this attempt will be discussed by comparison with the results obtained by using the above mentioned nonlinear differential equations.

If this treatment can be permitted, it will become possible to simplify the differential equations for solving the system transients.

However, in this treatment, as the power flow calculation is required in each time interval, the computing time for the stability studies increases.

2. Theory

2.1. Steady state characteristics of induction motor

The steady state equivalent circuit of induction motor is shown in Fig. 1. In this circuit, the following power equations are formulated (in per unit) ;

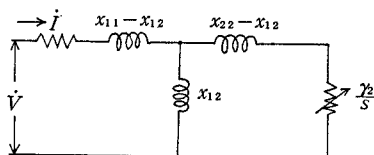


Fig. 1. Steady state equivalent circuit of induction motor.

* Kinki-Nippon Raylway Co., Ltd.

** Department of Electrical Engineering, College of Engineering.

$$P_M \cong \omega s T_z' \left(\frac{1}{x'} - \frac{1}{x} \right) V^2 \quad (1)$$

$$Q_M \cong \left\{ \frac{1}{x} + \frac{(\omega s T_z')^2}{x'} \right\} V^2 \quad (2)$$

where

P_M : input active power (synchronous watt)

Q_M : input reactive power (laggin)

ω : electrical angula velocity

s : slip

V : impressed voltage

$$x' = x_{11} - x_{12}^2 / x_{22}, \quad x = x_{11}$$

$$T_z' = \frac{x'}{x} T_0' \left(T_0' = \frac{x_{22}}{\omega r_2} \right), \quad (\omega s T_z')^2 \ll 1$$

The slip s in Ep. (1) and Eq. (2) is obtained by the next differential equation;

$$\frac{ds}{dt} = \frac{1}{M_u} (T_m - P_M) \quad (3)$$

$$T_m = T_0 \{ a(1-s)^{-1} + b(1-s)^0 + c(1-s)^2 \}$$

$$\cong T_0 \{ a(1+s) + b + c(1-2s) \}$$

T_m : mechanical torque

T_0 : mechanical torque at $s=0$

M_u : per unit inertia constant

a, b, c : rates of component of constant power torque, constant torque and diminishing torque in mechanical torque, respectively, and $a+b+c=1$

Therefore, steady state solution of slip equation is given as follows;

$$s \cong \frac{T_0}{k_T V^2 - T_0 (a-2c)} \quad (4)$$

where

$$k_T = \omega T_z' \left(\frac{1}{x'} - \frac{1}{x} \right)$$

Then, the power equations are obtained as follows, by substituting Eq. (4) into Eq. (1) and Eq. (2).

$$\left. \begin{aligned} P_M &\cong \frac{T_0 k_T V^2}{k_T V^2 - T_0 (a-2c)} \\ Q_M &\cong \left[\frac{1}{x} + \frac{1}{x'} \left\{ \frac{\omega T_0 T_z'}{k_T V^2 - T_0 (a-2c)} \right\}^2 \right] V^2 \end{aligned} \right\} \quad (5)$$

2.2. Power-voltage characteristics of the induction motor

The typical curves of P_m-V , Q_m-V which are obtained by using Eqs. (5), are shown in Fig. 2 and Fig. 3.

From these curves, it will be said that, for a small variation of the terminal voltage, Eqs. (5) can be approximated by the first order equations as follows;

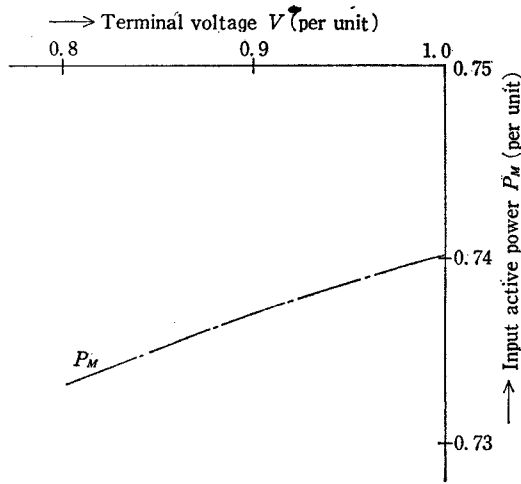


Fig. 2. Steady state active power characteristics of induction motor.

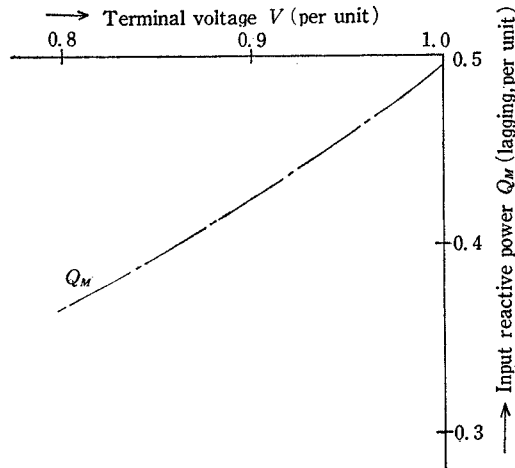


Fig. 3. Steady state reactive power characteristics of induction motor.

$$\left. \begin{aligned} P_M &= k_{ips}V + K_{ps} \\ Q_M &= k_{iqs}V + K_{qs} \end{aligned} \right\} \quad (6)$$

In this study, Eqs. (6) are adopted as the load characteristics of induction motor.

Coefficients of Eqs. (6), k_{ips} and k_{iqs} , are obtained through the use of partial derivatives of Eqs. (6) with respect to V .

$$k_{ips} = \frac{\partial P_M}{\partial V}, \quad k_{iqs} = \frac{\partial Q_M}{\partial V} \quad (7)$$

Constant terms of Eqs. (6), K_{ps} and K_{qs} , are decided from the steady state operating conditions of motor.

2.3. System analysis

The nodal equation which gives the current-voltage relation of a multi-machine system as shown in Fig. 4 is as follows;

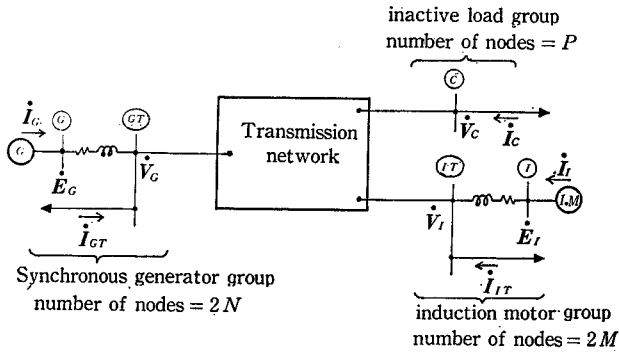


Fig. 4. A multi-machine system.

$$\begin{pmatrix} \dot{I}_G \\ \dot{I}_I \\ \dot{I}_{GT} \\ \dot{I}_{IT} \\ \dot{I}_C \end{pmatrix} = \begin{pmatrix} \dot{Y}_{N_{11}} & \dots & \dot{Y}_{N_{1n}} \\ \vdots & & \vdots \\ \dot{Y}_{N_{m1}} & \dots & \dot{Y}_{N_{mn}} \end{pmatrix} \begin{pmatrix} \dot{E}_G \\ \dot{E}_I \\ \dot{E}_G \\ \dot{E}_I \\ \dot{E}_C \end{pmatrix} \tag{8}$$

where

- \dot{E}_G, \dot{E}_I : internal voltage vector of generators and induction motors, respectively
- \dot{V}_G, \dot{V}_I : terminal voltage vectors of the same as the above
- \dot{V}_C : inactive load terminal voltage vector
- $\dot{I}_G, \dot{I}_{GT}, \dot{I}_I, \dot{I}_{IT}, \dot{I}_C$: Nodal-current vector shown in Fig. 4, respectively
- $\dot{Y}_{N_{ij}}$: element of node admittance matrix
- $n=2(M+N)+P$: total number of nodes

2.3.1. *The case that all induction motors are analyzed considering both mechanical and electrical transients*

In this case, the equations of the system machines are as follows; for induction motors,¹⁾

$$\left. \begin{aligned} \frac{d\dot{E}_{Ij}}{dt} &= -j\omega_0 s_j \dot{E}_{Ij} - \frac{1}{T'_{doj}} \left\{ \dot{E}_{Ij} - j(x_j - x'_j) \dot{I}_{Ij} \right\} \\ \frac{ds_j}{dt} &= \frac{1}{M_{tj}} (T_{mj} - P_{Mj}) \\ T_{mj} &= T_0 \{ a(1-s_j)^{-1} + b + c(1-s_j)^2 \} \\ P_{Mj} &= (\dot{E}_{Ij}^* \cdot \dot{I}_{Ij})_{real} \\ j &= 1, \dots, M \end{aligned} \right\} \tag{9}$$

where

- \dot{E}_{Ij} : internal voltage behind transient reactance x'_j
 - ω_0 : electrical angular velocity of power system in steady state
- for synchronous generators,

$$\left. \begin{aligned} \frac{d\theta_i}{dt} &= \omega_i \\ \frac{d\omega_i}{dt} &= \frac{\omega_0}{M_{Gi}} (P_{oi} - P_{ei}) \\ \dot{E}_{Gi} &= E_{Gi}(\cos \theta_i + j \sin \theta_i) \\ P_{ei} &= (\dot{E}_{Gi}^* \cdot \dot{I}_{Gi})_{real} \\ \text{where } \dot{E}_{Gi} &: \text{internal voltage behind transient reactance} \\ P_{oi} &: \text{mechanical input of No. } i \text{ generator} \end{aligned} \right\}$$

Moreover, when \dot{I}_{GT} , \dot{I}_{IT} and \dot{I}_C in Fig. 4 are constant impedance load's currents or some of these don't exist, Eq. (8) can be reduced as follows by eliminating disused nodes.

$$\begin{pmatrix} \dot{I}_G \\ \dot{I}_T \end{pmatrix} = \begin{pmatrix} \dot{Y}_{M_{11}} & \dots & \dot{Y}_{M_{1n}} \\ \vdots & & \vdots \\ \dot{Y}_{M_{m1}} & \dots & \dot{Y}_{M_{mm}} \end{pmatrix} \begin{pmatrix} \dot{E}_G \\ \dot{E}_I \end{pmatrix} \quad \text{where} \quad (10)$$

$m = N + M$

Numerical solutions of Eqs. (9) are obtained by applying Runge-Kutta method for each time interval using matrix equation (10).

2.3.2. *The case that some of the induction motors are analyzed by the first order equations of those terminal voltages*

This treatment should be adopted to the induction motors connected with the terminal which voltage variation is so small that the steady state solutions can be used. The number of differential equations for the induction motors in Eqs. (9) will be reduced by this treatment.

In this case, however, the terminal node currents \dot{I}_{GT} , \dot{I}_{IT} can not be eliminated, because the terminals connecting the induction motos become active terminals.

So, in this case, \dot{I}_G and \dot{I}_T are represented as follows;

$$\left. \begin{aligned} [\dot{I}_G] &= [\dot{Y}_G] [\dot{E}_G - \dot{V}_G] \\ [\dot{I}_T] &= [\dot{Y}_T] [\dot{E}_I - \dot{V}_I] \end{aligned} \right\} \quad (11)$$

where \dot{Y}_G , \dot{Y}_T : transient admittance matrices of generators and motors, respectively

and, in numerical calculation, terminal voltages concerned, \dot{V}_G or \dot{V}_I , must be decided for each time interval through power flow calculation.

3. Example system

One-line diagram of an example system is shown in Fig. 5.

In this system, nodes ①~③ are power plant buses, and nodes ④~⑥ are substation buses. In branches Δ and Δ , tap-changing transformers are set, and off-nominal turn ratios of these transformers are 1 : 1 in branch Δ , and 1 : 1.025 in Δ ⁴⁾.

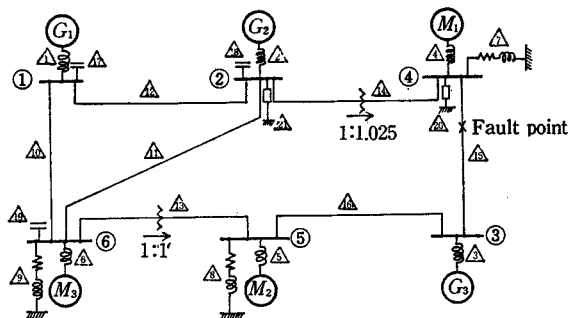


Fig. 5. Example system.

Each transmission line is a double-circuit. At each load terminal, an induction motor and a shunt impedance load are connected in parallel.

The ratio of power of induction motor load to shunt impedance load is as shown in Table 1. Transmission line impedances, each machine constants and operating conditions of the system are as shown in Table 2~Table 5.

Table 1. Rate of occupation of induction motor load.

Node number	Rate (%)
④	87
⑤	93
⑥	80

Table 2. Branch impedances. (p.u)

Branch number	Impedance
1	$j0.372$
2	$j0.260$
3	$j0.240$
4	$j0.166142$
5	$j0.466847$
6	$j0.302077$
7	} determined by motor outputs and designated load conditions
8	
9	
10	$0.123+j0.518$
11	$0.097+j0.401$
12	$0.080+j0.370$
13	$j0.300$
14	$j0.205$
15	$0.130+j0.189$
16	$0.052+j0.117$
17	$-j29.500$
18	$-j28.499$
19	$-j50.429$
20	$-j8.405$
21	$j8.000$

Table 3 Generator constants. (p.u)

Gen.	x_g	M
G_1	0.37	6.0
G_2	0.26	7.0
G_3	0.24	9.8

Table 4. Induction motor constants. (p.u)

Ind. motor	$r_1(=r_2)$	x_{11}	x_{22}	x_{12}	s	x	$T'do$	Mu
M_1	0.031097	2.76727	2.74912	2.6741	0.02414	0.166142	0.234492	4.0
M_2	0.087380	7.77580	7.72480	7.5140	∕	0.466847	∕	2.0
M_3	0.056540	5.03140	4.99840	4.8620	∕	0.302077	∕	3.0

Table 5 Designated operating conditions at each node point. (p.u)

Node	P	Q	V
①			1.05($\delta=0$)
②	0.30		1.04
③	0.50		1.10
④	-0.85	-0.20	
⑤	-0.30	-0.18	
⑥	-0.50	-0.05	

At the fault point in Fig. 5, the following three fault conditions are assumed;

- (1) three-phase short-circuit fault
- (2) one-circuit opening fault in double-circuit
- (3) double-circuit opening fault

In stability calculation, induction motors M_2 and M_3 are treated by the method described in 2.3.2, and induction motor M_1 is treated by the method 2.3.1, because induction motor M_1 is nearer to the fault point than the other two.

The results are compared with those which are obtained by treating all induction motor by the method 2.3.1, because the latter treatment will be given the accurate results.

4. Discussion of results

The results for three kinds of faults are shown in Fig. 6~Fig. 14, respectively.

In the cases of one-circuit opening and double-circuit opening fault, which are not so severe type fault, very accurate results are obtained because the internal voltage phase difference angles between generators swing in the maximum range of only 18 degrees and the terminal voltages of induction motors M_2 and M_3 only little vary.

While, in the case of three-phase short-circuit fault, which is a most severe type fault, there is some significant difference between the results from the precise

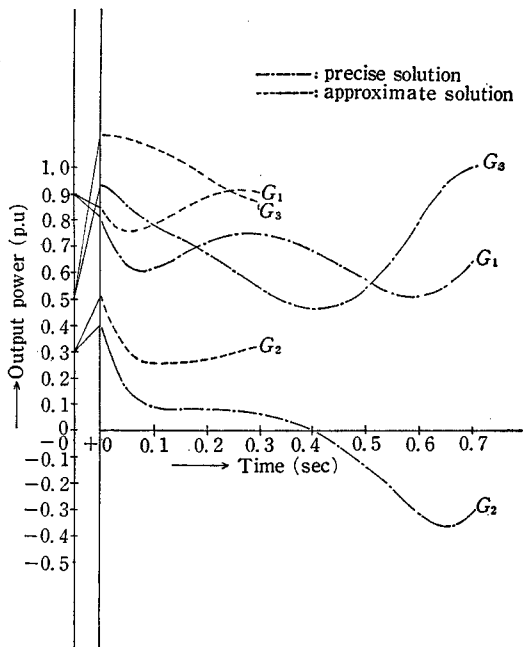


Fig. 6. Generator output power swings during three phase short circuit fault.

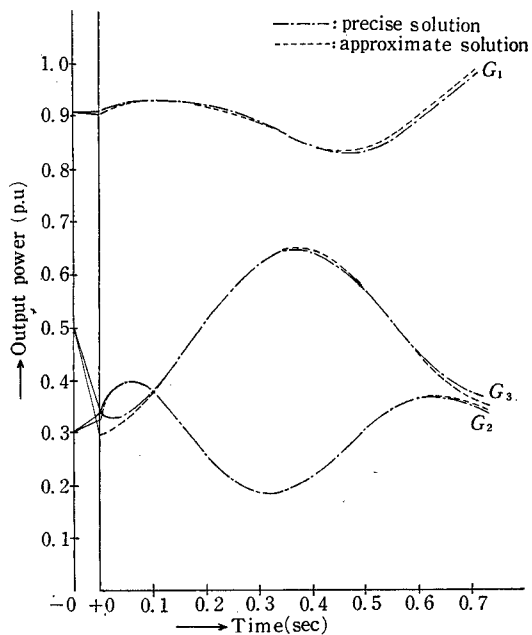


Fig. 7. Generator output power swings during double circuit opening fault.

treatment by 2.3.1 and the approximate treatment because the power swings are heavy and the terminal voltages vary very widely.

In results, the approximate treatment adopted here will give fairly precise

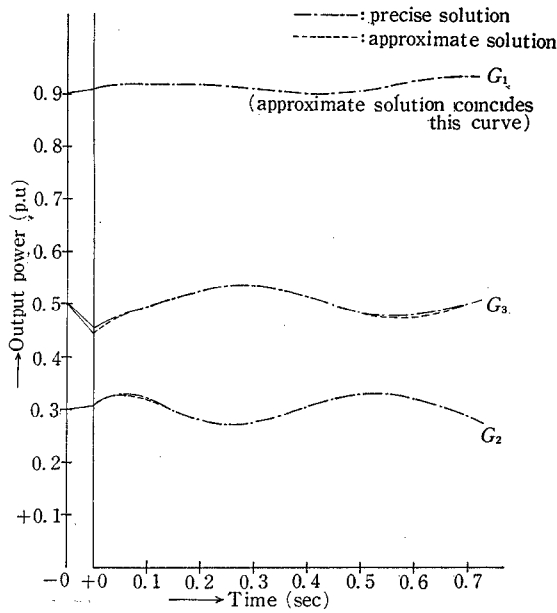


Fig. 8. Generator output power swings during one circuit opening fault.

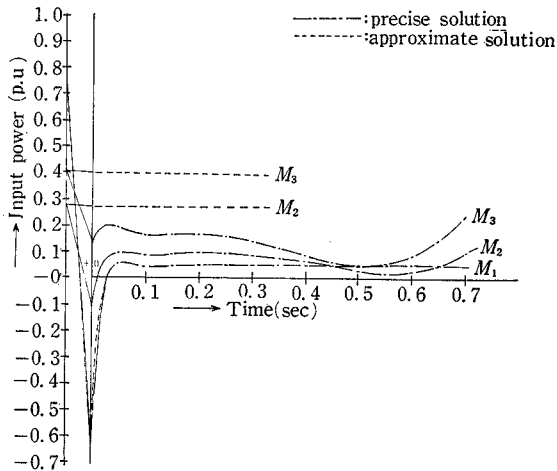


Fig. 9. Induction motor input power swings during three phase short circuit fault.

results in case of a less severe type fault, but can not be applied properly in such a fault that the voltage varies over a wide range.

5. Improved method for power flow calculation⁵⁾

5.1. Accelerating constant

In power flow calculation, successive relaxation (SR method) was applied. In this case, if the quantities which need some correction (for instance, voltages)

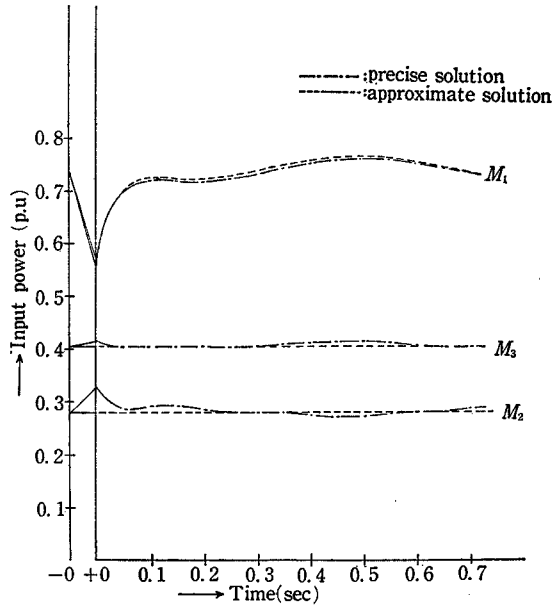


Fig. 10. Induction motor input power swings during double circuit opening fault.

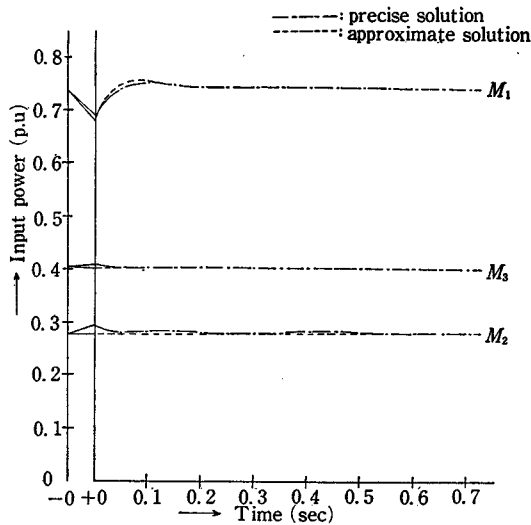


Fig. 11. Induction motor input power swings during one circuit opening fault.

decrease (or increase) by a nearly constant rate, in the process of calculation, an over correction, that is a procedure which multiply correction values by an accelerating constant at each iterative step, is practical. It is called "successive over relaxation method" (SOR method).

As it is recommended that the value of accelerating constant should be selected smaller than 2.0, the value is adopted to be 1.4 in this study.

The computing time for stability study by using SOR method could be reduced

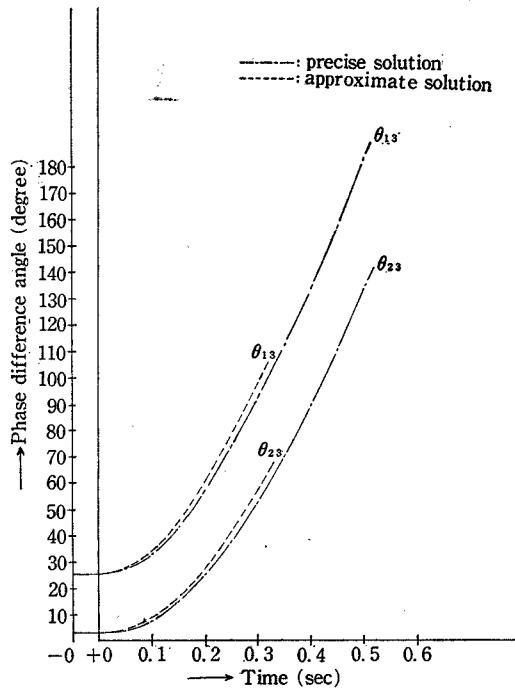


Fig. 12. Variations of internal voltage phase difference angle between generators during three phase short circuit fault.

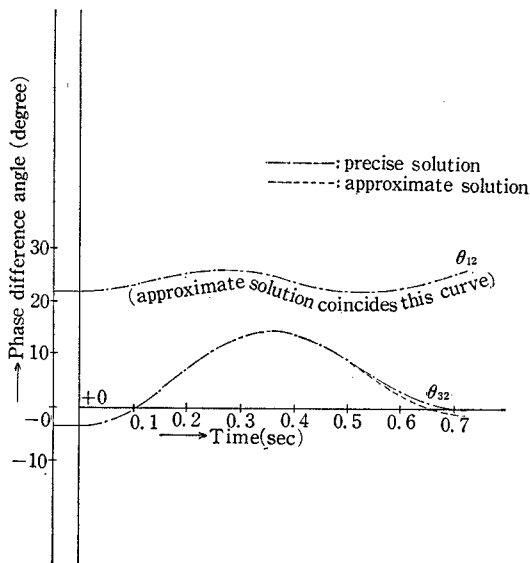


Fig. 13. Variations of internal voltage phase difference angle between during double circuit opening fault.

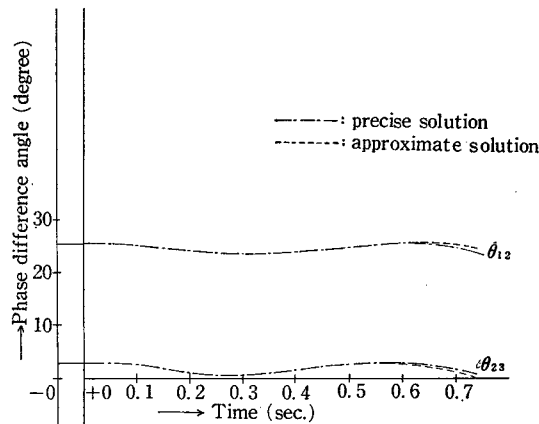


Fig. 14. Variations of internal voltage phase angle between generators during one circuit opening fault.

about 30 percent as compared with that by using SR method.

5.2. Current injection method

The convergence of power flow calculation depends on the admittance matrix form. In the case that the diagonal elements of admittance matrix are far larger than other elements, the convergence process is stable.

To make the diagonal elements large, there is a method, so called "current injection method", which is that an optional constant admittance is inserted at any load terminal and a proper current is injected at that terminal so as not to deviate from the designated terminal conditions.

The number of load terminals applied to this method is arbitrary.

In this study, this method was applied, but the speed of convergence was not improved by a reason that the eigen-values of the modified admittance matrix could not be made so small compared with that of the original admittance matrix.

6. Conclusion

It is clear from the discussion in Section 4 that the usefulness of representing the induction motor loads as the first order equations depends on the range of terminal voltage variation.

When the range of terminal voltage variation becomes greater than 20 percent, this treatment can not be used, and an appropriate range of terminal voltage variation, in which the precise results are expected, may be still narrower.

References

- 1) D. S. Brereton, D. G. Lewis and C. C. Young, *Trans. AIEE* **76**, pt. III, 451 (1957).
- 2) J. Baba, *Mitsubishi Denki Giho*, **32**, No. 11.
- 3) T. Taniguchi and M. Nakamura, *Trans. I.E.E.J.*, **92-B**, 37 (1972).
- 4) T. Taniguchi, Y. Azuma and M. Nakamura, *Bull. Univ. Osaka Pref. Ser. A*, **19**, No. 2 (1970).
- 5) Y. Sekine, *Analytical theory of power system*, p. 63, *Denki Shoin*, (1971).